

Alternative Nanostructures for Thermoacoustic Projectors: Carbonized Electrospun Nanofiber Sheets

Ali E. Aliev

A.G. MacDiarmid NanoTech Institute,
University of Texas at Dallas, Richardson, TX, 75083, USA
Ali.Aliev@utdallas.edu

ABSTRACT

Thermoacoustic performance of freestanding sheets of carbonized poly(acrylonitrile) nanofibers are studied as a promising candidate for thermophones. Spectral and power dependencies of sound pressure in air are compared with theoretical prediction. Thermodynamic properties of freestanding sheets analyzed using transport parameters of single nanofibers and their assembly in aligned and randomly deposited sheets. Electrical and thermal conductivities, thermal diffusivity, and infrared blackbody radiation response to short electrical pulses are examined to enhance the energy conversion efficiency. Applications of thermoacoustic projectors for loudspeakers, high power SONAR arrays, and sound cancellation are discussed.

Keywords: polymer nanofibers, electro-spinning, thermoacoustic sound generation, heat transfer

1 INTRODUCTION

Thermoacoustic (TA) sound generation using nanostructured materials, like carbon nanotube (CNT) sheets, graphene films and mechanically suspended metal nanowires has recently attracted much research interest because of possible practical importance. TA sound source requires low heat capacity per surface area and efficient heat exchange with the surrounding medium. Among the studied materials (carbon nanotube [1-3], graphene [4, 5], their sponges [6], PEDOT:PSS [7] and ITO films [8], porous silicon [9], and metal nanowire arrays [10]) CNT aerogel sheets provide the highest efficiency [6]. However, the limited accessibility of large-size freestanding carbon nanotube aerogel sheets, and other even more exotic materials recently investigated, hampers the field. The bundling of carbon nanotubes in large ropes of 100 - 150 nm and strong adhesiveness, are another drawback of small diameter carbon nanotubes for TA applications. We here describe alternative material for a thermoacoustic heat source with high energy conversion efficiency, additional functionalities, environmentally friendly and cost effective production technologies.

A poly(acrylonitrile) (PAN, $(C_3H_3N)_n$) is a strong, durable, and a thermally stable carbon-backbone polymer [11], that can be easily electrospun into random or highly aligned freestanding sheets. To make the organic fibers

suitable for thermoacoustic application the coating with gold, indium-tin-oxide and other metals (Bi_2Te_3 , Sb_2Te_3) have been proposed [6]. Despite of attractive performance as a thermophone heaters at low applied power, the increased heat capacity and limited temperature performance ($< 350^\circ C$) become main obstacles for coated PAN sheets. Here we propose another approach to make PAN nanofibers suitable for efficient TA sound generation without additional conducting coating - annealing of sheets with further carbonization. These measures turn the organic insulating fibers into mechanically strong highly conductive inorganic (or partially inorganic) nanofibers with reduced diameter and heat capacity [12]. By proper annealing the flexibility of fibers and sheets can be preserved.

Complete characterization of the thermodynamic properties of suitable nanostructured materials for TA transductions is challenging and requires sophisticated methods and apparatus: a thermal atomic force microscope, the 3-omega self-heating method, suspended micro-fabricated devices, micro-Raman, and so on. At the same time, the slope of sound pressure plotted versus frequency and applied ac power can explicitly characterize the heat source performance.

In the present work we thoroughly investigate the thermal, acoustical and energy conversion issues in TA projectors by seeking alternative heat source materials that provide additional functionality, are environmentally friendly and can be made using cost effective production technologies. We systematically study the spectral and power response of carbonized nanofiber sheets with different thicknesses, porosities and heat capacities, and analyze the effects of heat accumulation on the fundamental efficiency of TA sound generation. We provide extensive data base on thermal conductivity, thermal diffusivity, heat capacity and resistivity measurements combined with thermal imaging and dynamic infrared blackbody radiation response from the nanostructured heat surface.

2 RESULTS AND DISCUSSION

2.1. Annealed Poly(acrylonitrile) Nanofibers

The randomly electrospun and carbonized PAN (C-PAN) sheets shown in Fig. 1 with fiber diameters between 150 and 250 nm are mechanically robust and can withstand relatively high temperatures in air ($T = 600^\circ C$) and more

than 2000°C in vacuum or inert gases. The diameter of individual fibers, the thickness of the PAN sheet, and its areal density can be easily controlled by proper choice of a precursor solution (presently 10 wt% of PAN solution in N,N-dimethyl-acetamide, or DMF, $M_w = 150,000$), applied voltage (18-20 kV), distance between the spinning tip and set of counter electrode pillars, and spinning time [13, 14].

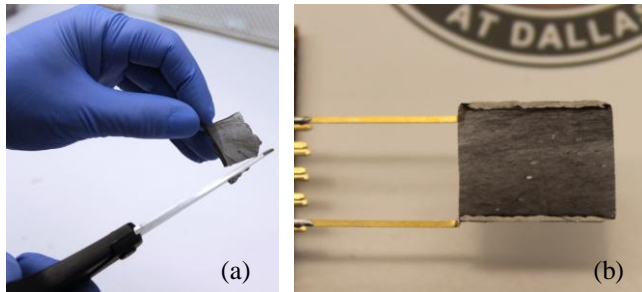


Fig. 1 (a) The self-supporting sheet of C-PAN nanofibers does not stick to touched surfaces and can be tailored by shears. (b) The 10x15 mm² C-PAN sheet attached to two gold-coated copper electrodes using silver paste.

Two set of fiber collectors were used to produce random and aligned sheets: revolving drum collector allowing continuous processing at collector speed of 300 rpm and vertically aligned set of two (or three) electrically connected or biased pillars. Developing carbon fiber from PAN based fiber is generally subjected to three processes namely stabilization, carbonization, and graphitization under controlled conditions. The stabilization at 280°C used in this work for 1 hour in air converts thermoplastic PAN to a non-plastic cyclic or a ladder compound and annealing in nitrogen furnace (N₂ / 5% H₂) for 1 hour at different temperatures (850 - 1100°C) turns it in to electrically conductive, mechanically strong C-PAN nanofibers with aspect ratio more than 10⁵. For further carbonization (graphitization) we used resistive heating of PAN sheets in high vacuum (~ 0.1 mTorr). The sequence of 10 short pulses of dc current were applied to the freestanding PAN sheet suspended between two gold-coated copper electrodes. The pulse width of 2 s was enough to measure the temperature of the sheet using infrared thermo camera FLIR T650sc (FLIR Systems, Inc.), but too short to deteriorate the silver paste, attaching the PAN sheet to the metal electrodes.

Smaller fiber diameters provide better uniformity in heat treatment and lower thermal inertia, which is important for thermoacoustic applications. Our observation of bundling in CVD grown multiwalled carbon nanotube forests and sheets via van der Waals forces suggest that the smallest diameter should exceed ~30 nm. Hence, in this work we search for nanofiber diameters ranging from 30 nm to 100 nm.

The self-supporting sheet of C-PAN shown in Fig. 1 (a, b) is optically transparent (> 50%), can be easily processed by hand, deployed (and removed) on any curved surfaces,

stretchable and tailored by shears. The freestanding C-PAN sheet can withstand strong air flow (the property which is very important at high sound pressure levels), vibrations and tensions. Unlike short CNTs (<0.5 mm), the length of electrospun fibers is terminated only on electrodes providing stable resistivity to the whole sheet.

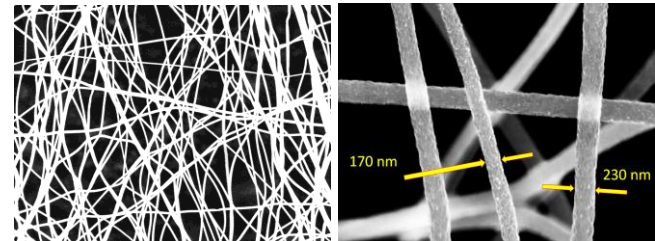


Fig. 2 SEM images of C-PAN sheet at increasing magnification.

The scanning electron microscope images in Fig. 2 taken by LEO 1530 VP, show relatively narrow distribution of C-PAN fiber diameters (170-230 nm) and homogeneous spreading of randomly aligned fibers in thin transparent sheets. The nanofibers do not show any trace of bundling. The length of individual fibers is the distance between pick up electrodes or last several centimeters for drum collector. Carbonization of post-annealed fibers by resistive heating does not significantly change the weight of sheet (~ 10 %) and diameter of fibers (260 nm → 230 nm). However, the resistance of sheets and fibers are reduced substantially.

2.2 Resistivity of nanofibers and sheets

The post-annealing (pyrolysis) makes organic insulating PAN fibers conductive at temperatures above 600°C (> 10 MΩ/□, □ denotes per square). The sheet resistance of 20 μm thick sheet is reduced three orders when annealed 1 hour at 800°C in nitrogen flow furnace (< 10 kΩ/□). The further carbonization by resistive heating in vacuum to 1300°C, and to 2000°C reduces the sheet resistance to another two orders of magnitude towards Ohmic range (in a below example from 29 kΩ to 280 Ω). It was suggested that the increase of conductivity results from the transformation of disordered carbons and isolated graphite structures to continuous graphite domains (graphitization). This process is a kinetically thermally activated process [15], therefore both, temperature and heat treatment time are important. The temperature dependencies of sheet resistance measured using 4-probe technique in Physical Property Measurement System (PPMS, Quantum Design Inc.) are shown in Fig. 3. The temperature gradient of resistance $R' = \Delta R/\Delta T$ and temperature coefficient of resistivity $TCR = (\Delta R/\Delta T)/R_{300}$ were estimated from the slope of $R(T)$ for given temperature range. Despite of significant change of resistance the slope of $R(T)$ is changed a little and remains negative at room temperature, which is typical for carbon materials (non-

metals) with low concentration of free electron carriers, $\text{TCR} = (-2.9 \rightarrow -1.0) \times 10^{-3} \text{ K}^{-1}$.

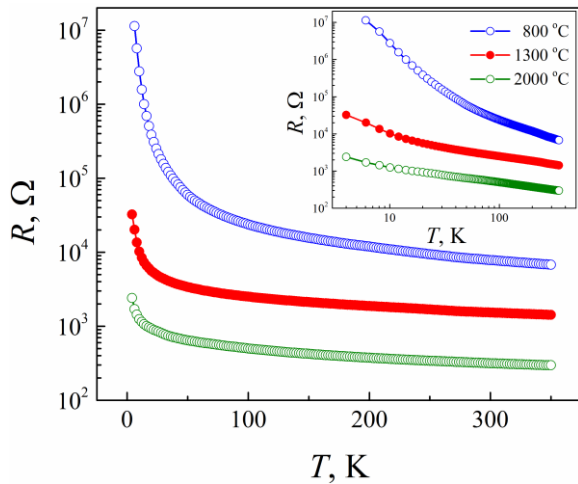


Fig. 3 The temperature dependence of resistance for PAN sheet post annealed in nitrogen ($\text{N}_2/5\%\text{H}_2$) furnace at 800°C for 1 hour (open blue circles), resistively heated in vacuum to 1300°C (solid red circles), and further resistively heated in vacuum to 2000°C (open green circles). Inset shows the change of $R(T)$ slopes in logarithmic scale.

2.3 Thermal conductivity and thermal diffusivity of C-PAN nanofibers and sheets.

The thermal conductivity and the thermal diffusivity measurements of C-PAN single nanofibers and sheets were performed using a self-heating 3-omega technique. For this the independent determination of electrical resistivity and the temperature gradient of resistance were performed for each temperature interval. These measurements provide complementary information for the thermal transport and can be easily combined within one setup.

3-omega method. The nanoscale dimension of free-standing C-PAN fibers interwoven in thin ($\sim 20 \mu\text{m}$) aerogel network of C-PAN sheet suggests the use of the self-heating 3-omega technique to determine the thermal transport along the narrow strip of sheet, or individual fiber. In this case, the one-dimensional heat flow along the sheet (fiber) can be expressed in the terms of the third-harmonic (3ω) voltage signal $U_{3\omega}$ induced by an ac current $I_0 \cdot \sin \omega t$ applied through the elongated sample (the aspect ratio of sample should be >100) [16].

C-PAN sheets. The measured thermal conductivity of the sheet is gradually increases in a wide temperature range (see Fig. 4(a)). The heat treatment in vacuum increases the thermal conductivity of sheet two fold by annealing at 1300°C and to one order by annealing at 2000°C.

The heat capacity of the sheet can be estimated from the known thermal conductivity, κ and thermal diffusivity, α , $C_p = \kappa/\alpha\rho \approx 600 \text{ J/kg}\cdot\text{K}$, where $\rho \approx 120 \text{ kg/m}^3$ is the density of the sheet having porosity of 91.5 % (estimated from SEM images). The obtained value of C_p is typical for

carbonized fibers (note, for graphite $C_p = 716 \text{ J/kg}\cdot\text{K}$ at $T = 295 \text{ K}$).

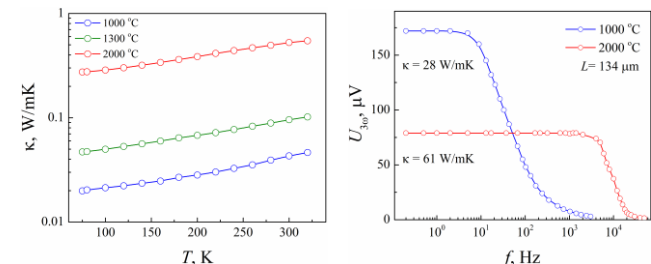


Fig. 4 (a) The temperature dependence of thermal conductivity of freestanding PAN sheet post annealed at 1000°C in nitrogen atmosphere (blue open circles), carbonized in vacuum at 1300°C (green open circles), and carbonized at 2000°C (open red circles). (b) The frequency dependence of third-harmonic signal for single PAN fiber post-annealed at 1000°C (blue open circles, $R_0 = 198 \text{ k}\Omega$), and the same fiber resistively heated to 2000°C (red open circles, $R_0 = 22.3 \text{ k}\Omega$). $L = 0.134 \mu\text{m}$, $D = 250 \mu\text{m}$, $T = 295 \text{ K}$.

Individual Fibers. The frequency dependencies of third-harmonic signals (shown in Fig. 4(b)) and the slope of phase delay were measured for an individual nanofiber, annealed at 1000°C and then heat treated *in situ* in vacuum at 2000°C are. The thermal conductivity extracted from the low-frequency shoulder of $U_{3\omega}(f)$ shows 2 fold increase ($28 \rightarrow 61 \text{ W/mK}$), while the thermal diffusivity obtained from the slop of phase delay, shows more than two orders of increase ($0.66 \rightarrow 106 \text{ mm}^2/\text{s}$). The significant increase of the thermal diffusivity in single nanofibers perhaps due to partial crystallization of carbonaceous stuff (increase of phonons mean-free-path) and decrease of fiber density, ρ (lost of mass), and heat capacity, C_p (crystallization reduces the number of phonons): $\alpha = \kappa/\rho C_p$. The decrease of thermal inertia, ρC_p , can enhance the heat exchange coefficient of whole sheet and improve the thermoacoustic performance of the device.

2.3 Thermoacoustic performance

The different thickness of C-PAN mats, self-supporting sheets, and thin transparent aerogel type webs with electrical sheet resistances from 100Ω to $20 \text{ k}\Omega$ were tested. The spectra and power dependencies of sound pressure were measured in near field, $r = 3 \text{ cm}$, at room temperature in air. The details of experimental setup are described elsewhere [6]. The bulk blue circles in Fig. 6(a) are for the large ($3.3 \times 3.3 \text{ cm}^2$) C-PAN sheet with the thickness of $120 \mu\text{m}$, bulk red circles are for $1.2 \times 1.2 \text{ cm}^2$, $h = 120 \mu\text{m}$, and bulk green circles are for $1.2 \times 0.9 \text{ cm}^2$, $h = 60 \mu\text{m}$ (the $120 \mu\text{m}$ mat was split to two plates with thickness of $60 \mu\text{m}$), respectively. The sound pressures are normalized to the applied ac power, $P_h = 1.72 \text{ W}$, 2.78 W , and 1.08 W , respectively. The observed low sound pressure level generated by thick mats apparently due to the heat

accumulation and low heat exchange coefficient. The relatively higher sound pressure at low frequencies measured from large mat is due to the better matching to near field conditions at a distance of 3 cm. However, at frequencies > 60 kHz this size of projectors creates strong interference of sound coming from the edges and central part of the mat. For smaller C-PAN mats the interference region is shifted to higher frequencies.

Six fold increase of sound pressure was observed when the thickness of annealed PAN sheet decreased to ~ 20 μm . This thin transparent web-type sheet shows promises for wide-band TA projectors. The green dashed line in Fig. 6(a) show the theoretical line calculated using Equation 1 in [6]. The sound pressure versus applied ac power for thick 120 μm porous mat is declined from linear increase at relatively low power and follows the temperature profile measured on the surface of heater by FLIR thermocamera. For thin sheet the $p(P_h)$ dependence is more linear suggesting better heat dissipation and higher exchange coefficient with surrounding air. The temperature coefficient of resistivity $\alpha = (\Delta R / \Delta T) / R_{300}$ for this thin film, estimated from the slope of $R(T)$ at room temperature, is negative and typical for carbon materials (non-metals), $-2.6 \times 10^{-3} \text{ K}^{-1}$.

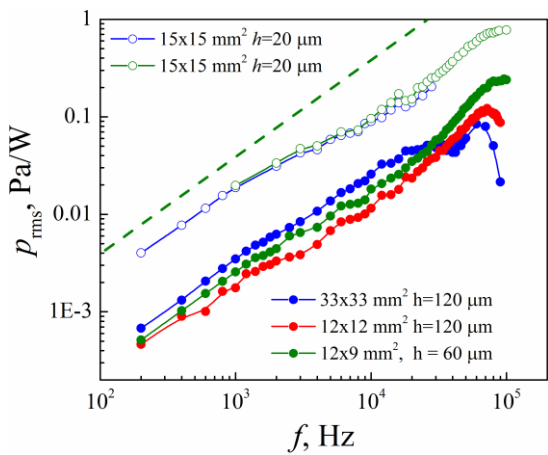


Fig. 5 (a) The sound pressure spectra of thick mats (bulk circles) and thin transparent sheets (open circles) of C-PAN nanofiber sheets annealed at 1000°C.

The low-density C-PAN nanofiber aerogel sheet provides high performance as a TA heat source in open air up to 140 kHz. Despite the high thermal inertia of large diameter PAN fibers (170-230 nm), which decreases the overall performance of the TA heater comparing to theoretical line, the open aerogel structure of the thin C-PAN sheet provides enhanced heat exchange and a broad power range where sound pressure linearly increases versus applied power.

3 CONCLUSIONS

The carbonized PAN sheets have several attractive features as an alternative material for thermoacoustic projector applications: (i) freestanding sheets of C-PAN

fibers resample an aerogel type structure of carbon nanotube sheet with high surface area and enhanced heat exchange coefficient with surrounding air, (ii) no bundling issues was observed, (iii) easy to handle, enviromently frendly, and has low cost technology.

The large diameter distribution and inhomogeneity of density of fibers in electrospun sheets substantially reduces the TA performance: large diameter fibers, owing low electrical resistance, create the current redistribution, like in bundled CNT sheets; higher local density of fibers creates accumulation of heat in those areas with relatively higher temperature, leading to further reduction of resistance and current redistribution.

The pyrolysis of PAN sheets in inert gases, which preserves the mechanical strength and decreases the fiber diameter, is a promising route to improve the TA performance of the heater. The further work needed to improve the performance of PAN derived TA heaters, namely the diameter of fibers should be reduced twice by proper choice of solution and applied electrostatic potential. The resistance of fibers can be decreased by increasing the carbonization temperature and doping.

REFERENCES

1. L. Xiao, et al. Nano Lett. 8, 4539, 2008.
2. A. E. Aliev, M. D. Lima, S. Fang, R. H. Baughman, Nano Lett. 10, 2374, 2010.
3. A. E. Aliev, Y. N. Gartstein, R. H. Baughman, Nanotechnology 24, 235501, 2013.
4. H. Tian, et al. ACS Nano 5, 4878, 2011.
5. J. W. Suk, K. Kirk, Y. Hao, N. A. Hall, , R. S. Ruoff. Adv. Mater. 24, 6342, 2012.
6. A. E. Aliev, et al. ACS Nano 9 (5), 4743, 2015.
7. H. Tian, et al. Appl. Phys. Lett. 99, 233503, 2011.
8. H. Tian, et al. Appl. Phys. Lett. 99, 043503, 2011.
9. H. Shinoda, T. Nakajima, K. Ueno, N. Koshida, Nature 400, 853, 1999.
10. A. O. Niskanen, J. Hassel, M. Tikander, P. Maijala, L. Grönberg, P. Helistö, Appl. Phys. Lett. 95, 163102, 2009.
11. M. S. A. Rahaman, A. F. Ismail, A. A. Mustafa, Polym. Degrad. Stab. 92, 1421, 2007.
12. Y. Wang, et al. IEEE Transactions on nanotechnology 2, 1, 39, 2003.
13. S. Ramakrishna, K. Fujihara, W. E. Teo, T. C. Lim, Z. Ma, "An Introduction to Electrospinning and Nanofibers," Singapore: World Scientific, 2005.
14. A. Frenot, I. S. Chronakis, Current Opinion in Colloid and Interface Science 8, 64, 2003.
15. N. Bhardwaj and S. C. Kundu. Biotechnol. Adv. 28, 325, 2010.
16. L. Lu, W. Yi, D. L. Zhang, Review of Scientific Instruments 72, 2996, 2001.